The ATPase activity of MLH1 is required to orchestrate DNA double-strand breaks and end processing during class switch recombination

Richard Chahwan,[1] Johanna M.M. van Oers,[1] Elena Avdievich,[1] Chunfang Zhao,[1] Winfried Edelmann,[1] Matthew D. Scharff,[1] and Sergio Roa[1,2]

[1]Department of Cell Biology, Albert Einstein College of Medicine, Bronx, NY 10461
[2]Oncology Division, Center for Applied Medical Research, University of Navarra, 31008 Pamplona, Spain

Antibody diversification through somatic hypermutation (SHM) and class switch recombination (CSR) are similarly initiated in B cells with the generation of U:G mismatches by activation-induced cytidine deaminase but differ in their subsequent mutagenic consequences. Although SHM relies on the generation of nondeleterious point mutations, CSR depends on the production of DNA double-strand breaks (DSBs) and their adequate recombination through nonhomologous end joining (NHEJ). MLH1, an ATPase member of the mismatch repair (MMR) machinery, is emerging as a likely regulator of whether a U:G mismatch progresses toward mutation or DSB formation. We conducted experiments on cancer modeled ATPase-deficient MLH1G67R knockin mice to determine the function that the ATPase domain of MLH1 mediates in SHM and CSR. *Mlh1*$^{GR/GR}$ mice displayed a significant decrease in CSR, mainly attributed to a reduction in the generation of DSBs and diminished accumulation of 53BP1 at the immunoglobulin switch regions. However, SHM was normal in these mice, which distinguishes MLH1 from upstream members of the MMR pathway and suggests a very specific role of its ATPase-dependent functions during CSR. In addition, we show that the residual switching events still taking place in *Mlh1*$^{GR/GR}$ mice display unique features, suggesting a role for the ATPase activity of MLH1 beyond the activation of the endonuclease functions of its MMR partner PMS2. A preference for switch junctions with longer microhomologies in *Mlh1*$^{GR/GR}$ mice suggests that through its ATPase activity, MLH1 also has an impact in DNA end processing, favoring canonical NHEJ downstream of the DSB. Collectively, our study shows that the ATPase domain of MLH1 is important to transmit the CSR signaling cascade both upstream and downstream of the generation of DSBs.

CORRESPONDENCE
Matthew D. Scharff:
matthew.scharff@einstein.yu.edu
OR
Sergio Roa:
sroa@unav.es

Abbreviations used: AID, activation-induced cytidine deaminase; ChIP, chromatin immunoprecipitation; CSR, class switch recombination; DSB, double-strand break; MMR, mismatch repair; NHEJ, nonhomologous end joining; SHM, somatic hypermutation; SR, switch region.

A diverse repertoire of high affinity antibodies is required to protect us from foreign antigens. To create such a repertoire, Ig genes in germinal center B cells undergo a high rate of somatic hypermutation (SHM) and class switch recombination (CSR) that lead to the affinity maturation and isotype switching required to generate protective antibodies. These processes are initiated by activation-induced cytidine deaminase (AID), which converts dC to dU in single-stranded DNA (Maul et al., 2011; Stavnezer, 2011). The U:G mismatches created by AID lead to transition mutations through replication or to the recruitment of error-prone base excision repair and mismatch repair (MMR) proteins that introduce additional mutations at the Ig locus (Stavnezer, 2011). Although MMR normally maintains the integrity of the genome, at the Ig genes, it paradoxically mediates extensive mutation and the formation of DNA double-strand breaks (DSBs) at specific switch regions (SRs; Chahwan et al., 2011).

MMR is mainly mediated by two protein complexes: MutSα (MSH2 and MSH6), which identifies the DNA mismatch, and MutLα

The Rockefeller University Press $30.00
J. Exp. Med. Vol. 209 No. 4 671-678
www.jem.org/cgi/doi/10.1084/jem.20111531

(MLH1 and PMS2), which signals downstream effector functions (Kunkel and Erie, 2005; Iyer et al., 2006; Jiricny, 2006). Both complexes appear equally crucial for the global repair of DNA mismatches, yet their roles in mediating antibody diversity differ. The MutSα complex is required for both SHM and CSR (Chahwan et al., 2011), whereas MutLα seems to function only during CSR (Kim et al., 1999; Phung et al., 1999; Schrader et al., 1999; Ehrenstein et al., 2001; Péron et al., 2008; Stavnezer et al., 2010; van Oers et al., 2010). Although the processes of SHM and CSR are similar in their initial phases because both are triggered by AID-generated U:G mismatches, their outcomes differ in that during CSR, those mutations lead to DSBs that must then be resolved by nonhomologous end joining (NHEJ; Kotnis et al., 2009). The activation of the latent endonuclease activity of PMS2 in MutLα complexes contributes to the generation of those DSBs (van Oers et al., 2010). MLH1, as the protein that directly interacts with the mismatch sensor MutSα, anchors the MutL complexes (Kunkel and Erie, 2005; Iyer et al., 2006; Jiricny, 2006) and is required for the recruitment of PMS2 and its endonuclease activity during CSR (Cannavo et al., 2007; van Oers et al., 2010).

MLH1 is a candidate factor to orchestrate the different roles of MutLα in SHM and CSR because it coordinates the MMR process through its physical interactions with the MMR core proteins and through its ATPase activity modulates the timing and spatial relationships of the activities of the MMR complex (Polosina and Cupples, 2010). The interactome of MLH1 has been shown to contain proteins involved not only in MMR but also in DNA metabolism and repair, among other functions (Cannavo et al., 2007), supporting its role in orchestrating many downstream processes. MLH1 belongs to the GHL (or HATPase) family of ATPases (Ban et al., 1999; Hu et al., 2003), which features a noncanonical ATP-binding domain (Bergerat et al., 1997). Inactivating mutations, primarily in the conserved N terminus of hMLH1 or loss of expression of hMLH1, are among the most frequent causes of Lynch (HNPCC [hereditary nonpolyposis colorectal cancer]), Muir-Torre, and Turcot (HNPCC variant) cancer syndromes (Shah et al., 2010). The recurrent G67R mutation in hMLH1 is located in one of the GxG motifs of the ATPase domain (Fig. 1 A). This particular mutation does not prevent its interaction with PMS2 to form MutLα complexes, but it does impede DNA repair functions and promote a strong cancer phenotype (Raevaara et al., 2005; Avdievich et al., 2008).

A recently generated mouse model carrying the MLH1G67R mutation and expressing almost normal protein levels showed a separation of function phenotype, exhibiting inactive DNA repair functions and infertility but retaining DNA damage responses involving cell cycle arrest and apoptosis (Avdievich et al., 2008). In addition, MLH1GR mice differed from null mice in their tumor spectrum and frequency. Because G67R retains the interaction of MLH1 with PMS2 (Raevaara et al., 2005; Avdievich et al., 2008) and does not affect its apoptosis signaling (Avdievich et al., 2008), MLH1GR mice provide a unique opportunity to study the impact of its ATPase activity on the multiple functions of MLH1 during SHM and CSR. We show here that although SHM is not affected by the loss of the ATPase activity of MLH1, CSR is dramatically impaired. The ATPase-dependent functions of MLH1 promote the generation of DSBs that are necessary during CSR and ultimately influence the NHEJ mechanisms that repair such DSBs at the SRs.

RESULTS AND DISCUSSION

Normal SHM in *Mlh1*$^{GR/GR}$ mice

A highly conserved GxG sequence motif (Fig. 1 A) is located in the loops defining the boundary of the ATP binding pocket of bacterial MutL (Dutta and Inouye, 2000). The mammalian MLH1 ATP binding pocket behaves similarly in a crystal structure resolved at 2.5 Å (Protein Data Bank accession no. 3NA3; Fig. 1 A). Accordingly, the GxG motif is in a polypeptide stretch devoid of secondary structures, suggesting that a G67R mutation should not significantly affect the overall integrity of the ATPase or the adjacent MutS interaction domains. However, G67 appears to be in close proximity to the adenine base of the ATP molecule (Fig. 1 A), suggesting that a G67R mutation could greatly alter the bulkiness and charge of the ATP pocket, thereby hindering the accommodation of the ATP molecule.

ATP binding and/or hydrolysis by the ATPase of MLH1 is believed to induce large conformational changes (Sacho et al., 2008; Johnson et al., 2010) capable of mediating an MMR signaling cascade by recruiting and activating downstream effector proteins after MutS‘ binding (Ban et al., 1999; Dutta and Inouye, 2000; Spampinato and Modrich, 2000; Tomer et al., 2002; Chahwan et al., 2011). Although MLH1 and its ATPase activity are required for efficient DNA MMR in vitro and in vivo (Räschle et al., 2002; Tomer et al., 2002; Jiricny, 2006; Avdievich et al., 2008), there has been some uncertainty about the role of MLH1 in the resolution of the AID-generated mismatches during SHM. In fact, the frequency and characteristics of mutations in MLH1-deficient mice were previously shown to be altered in an artificial exogenous transgene but normal when an endogenous Ig variable gene was studied in knockout mice (Kim et al., 1999; Phung et al., 1999). To determine whether the continued presence of the protein but the loss of the ATPase activity of MLH1 had any effect on SHM, three WT and three *Mlh1*$^{GR/GR}$ mice were immunized with NP_{36}-CGG to promote SHM in the rearranged V_H186.2 gene. We found no significant differences in the overall mutation frequencies between WT and *Mlh1*$^{GR/GR}$ mice ($P = 0.4252$; Fig. 1 B), and the distribution of mutations was similar ($P \geq 0.0576$; Fig. 1 C). Although there was a slight tendency for more G:C mutations in mutant mice, the number of transversions or transitions ($P \geq 0.2652$), the different types of substitutions ($P \geq 0.0576$), and the cumulative spectrum of mutations from G, C, A, or T sites ($P \geq 0.2183$) were also comparable between WT and mutant mice (Fig. 1, B and D). Furthermore, the overall mutation frequencies of the hotspots for AID

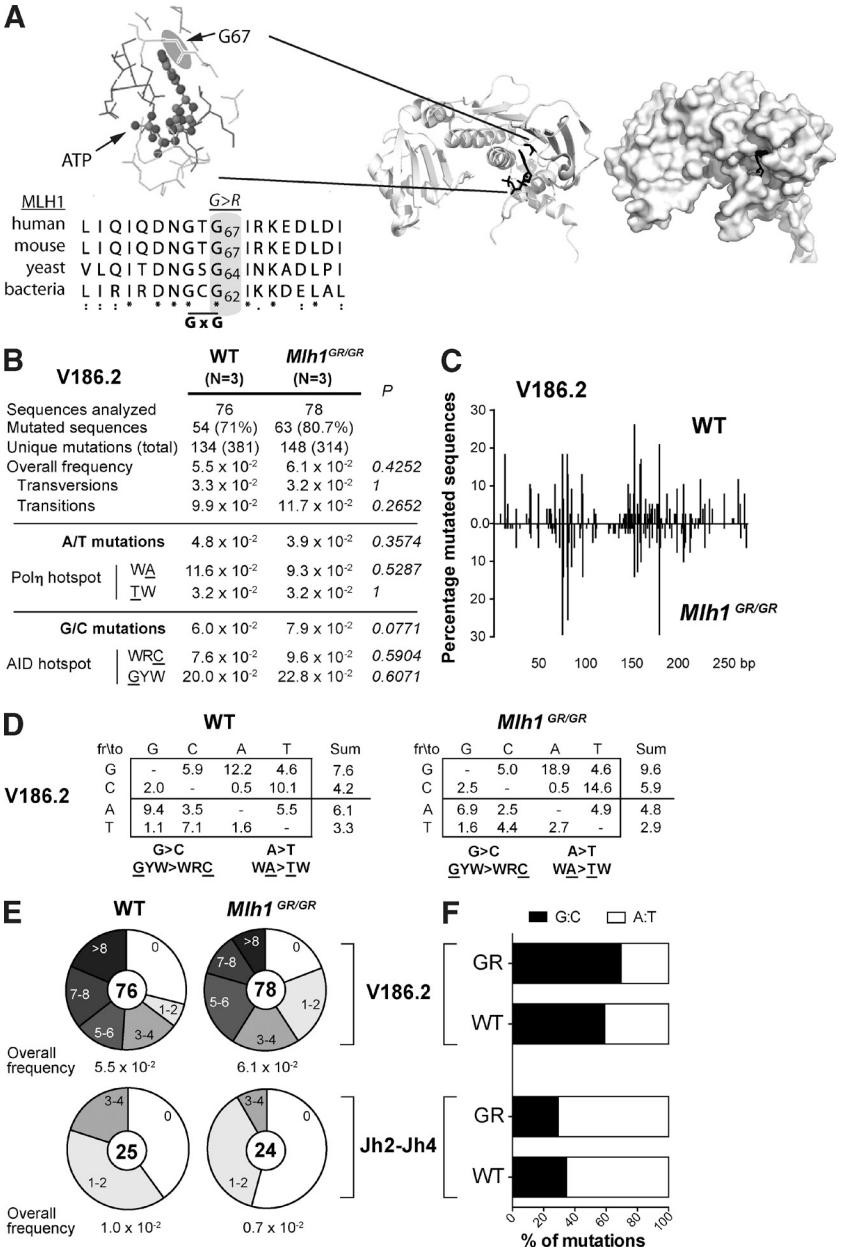

Figure 1. The MLH1G67R mutation does not have a significant impact on SHM. (A) Alignment of the GxG motif of MLH1 ATPase domain and a 2.5-Å resolution of the backbone of hMLH1 ATP-binding pocket with ATP (Protein Data Bank accession no. 3NA3). G67 of human MLH1 is highlighted with a gray oval, and the ATP molecule is shown inside the MLH1 ATPase pocket. Asterisks signify that the amino acid conservation is identical, and colons signify similarity at the respective amino acid residues. On the right, a cartoon backbone and a surface representation of the first 347 aa residues of mammalian MLH1 along with an ATP molecule trapped in the ATPase domain are shown. The G67 residue does not seem to be in a region having secondary structures but is in close proximity to the adenine base of the ATP molecule and not to the triphosphate group. Although MLH1 was crystallized as a homodimer, for simplicity, only the monomer is shown here. (B) Global analysis of unique mutation frequencies corrected for base composition according to the SHMTool algorithm. (C) Distribution of mutations in the V_H186.2 sequence (273 bp). (D) The spectrum of base substitutions is expressed as frequencies of mutation ($x10^{-2}$ mutations/base) and corrected for base composition. The cumulative spectrum of mutations from G, C, A, or T sites is also shown (Sum). (E) Proportion of sequences with different load of mutations (indicated in each fraction) for antigen and nonantigen selected regions (V_H186.2 and Jh2-Jh4, respectively). The center of the pies represents the total number of sequences analyzed in each group. (F) Relative frequency of mutations at G:C versus A:T sites observed in V_H186.2 and Jh2-Jh4 regions.

(WRC/GYW) and Polη (WA/TW), which are major hallmarks of the SHM process, were similar in both groups ($P \geq 0.5287$; Fig. 1 B). Finally, the strand bias signatures previously reported in antigen-selected V(D)Js (Steele, 2009; Roa et al., 2010; van Oers et al., 2010), which show WA>TW and GYW>WRC biased frequencies, were similarly evident in both WT and *Mlh1*$^{GR/GR}$ mice (Fig. 1, B and D). To determine whether selection pressures on the V_H186.2 coding region concealed hypermutation differences, we compiled unique mutations within the intronic Jh2-Jh4 region of splenic B cells from unimmunized mice. As expected, Jh2-Jh4 sequences yielded fewer mutations than V_H186.2 sequences (Fig. 1 E), but the overall mutation frequencies and the relative spectrum of mutations in both scenarios were comparable between the mutant and WT mice (Fig. 1, E and F). Fig. 1 F also shows a difference in G:C/A:T ratios between V_H186.2 and Jh2-Jh4 regions, an observation which is not completely understood yet but has been connected before to intrinsic differences between antigen and nonantigen selected regions (Steele, 2009).

Other MMR factors, including MutSα, the exonuclease EXO1, the ubiquitylated form of PCNA, and error-prone polymerases such as Polη, have been clearly shown to behave as error-prone factors at the Ig locus, modifying the spectrum of substitutions and introducing mutations at A:T sites within the V (variable) region (Chahwan et al., 2011). However, our data here on the catalytic mutant MLH1 expand previous findings that show little or no effect of MLH1 (Kim et al., 1999; Phung et al., 1999) or PMS2 deficiency (Péron et al., 2008; van Oers et al., 2010) in SHM of B cells. The reason why the heterodimer MLH1–PMS2 collaborates with MSH2/MSH6/PCNA/EXO1/Polη outside the V region and is essential in global MMR but seems to be irrelevant for SHM remains unknown. It is likely that there is some mechanism to prevent MutLα from being recruited by the MutSα complex or

becoming active at the V region so as to prevent it signaling for additional downstream elements and reduce the likelihood of DSBs.

Mlh1$^{GR/GR}$ B cells show reduced efficiencies of CSR

In contrast to the lack of a significant effect of the loss of MLH1 and of its ATPase activity on SHM, *Mlh1*$^{-/-}$ mice have a substantial decrease in CSR (Schrader et al., 1999; Stavnezer et al., 2010; Eccleston et al., 2011). Because this decrease in CSR could be caused by the absence of the MLH1–PMS2 complex, including its scaffolding functions, or by the loss of the ATPase activity of MLH1, we examined whether the selective inactivation of the ATPase activity of MLH1 would affect CSR. We purified splenic B cells from mutant and WT mice and stimulated them with LPS or with LPS + IL4 to induce ex vivo switching from IgM to IgG3 and IgG1, respectively. After normalization of the efficiencies of switching to WT levels, *Mlh1*$^{GR/GR}$ mice showed an ∼70% reduction in CSR to all studied isotypes ($P < 0.001$; Fig. 2, A and B). No appreciable differences in proliferation that might delay CSR were detected between WT and *Mlh1*$^{GR/GR}$ B cells, as assessed by CFSE dilution histograms (Fig. 2 C).

A similar phenotype has been shown in the absence of PMS2, an essential partner of MLH1 during CSR and postreplicative MMR (Schrader et al., 1999; Ehrenstein et al., 2001; Péron et al., 2008; van Oers et al., 2010). These reduced efficiencies in CSR have been associated with impaired generation and resolution through NHEJ of DSBs, both of which are critical for CSR (Stavnezer et al., 2010). However, little is known about the functional domains of MLH1 and the role, if any, of its distinct catalytic activities during CSR. Based on the deficiency in CSR exhibited here by *Mlh1*$^{GR/GR}$ B cells, it became plausible to explore the hypothesis that the ATPase activity of MLH1 might play a role in the generation and/or resolution of the DSBs produced during CSR.

The generation of DSBs is decreased in *Mlh1*$^{GR/GR}$ activated B cells

Because MLH1–PMS2 ATPase activities are thought to be required for the activation of the MutL endonuclease function (Pillon et al., 2010; Polosina and Cupples, 2010) leading to DSBs in SRs (van Oers et al., 2010), we determined whether DSB generation during B cell activation was affected in *Mlh1*$^{GR/GR}$ mice. To examine whether there was a specific decrease of DSBs at SRs, chromatin immunoprecipitation (ChIP) experiments using anti-53BP1 antibodies were conducted on activated B cells from WT, *Mlh1*$^{-/-}$, and *Mlh1*$^{GR/GR}$ mice. 53BP1 has been shown to be essential for CSR and the mediation of DNA end joining (Ramachandran et al., 2010; Bothmer et al., 2011), and therefore the recruitment of 53BP1 to the targeted SRs serves as a reporter for the presence of DSBs. As expected, 53BP1 protein was enriched approximately two- to fourfold on the Sμ and Sγ1 region in LPS + IL4–stimulated WT B cells compared with the respective *Mlh1*$^{-/-}$ or *Mlh1*$^{GR/GR}$ (Fig. 3 A). We did not find a significant increase on the Sγ3 region, which switches infrequently after LPS + IL4 treatment (Stavnezer et al., 2010), suggesting that the observed 53BP1 enrichment was specific. Furthermore, we used Western blots to examine the levels of H2AX that undergo rapid phosphorylation (γ-H2AX) in response to the generation of DSBs in the stimulated B cells (Rogakou et al., 1999). As expected, all cells stimulated with LPS or with LPS + IL4 had considerably higher γ-H2AX signal compared with nonstimulated cells (Fig. 3 B). However, the increase in the overall amount of γ-H2AX was much lower in activated *Mlh1*$^{GR/GR}$ splenic B cells than in WT cells (Fig. 3 B), also suggesting a smaller accumulation of DSBs in the mutant cells.

Collectively, these data suggest that there is a decrease in the formation of DSBs in the relevant SRs in the MLH1-ATPase mutant B cells that is comparable with that found in mice lacking MLH1. This is consistent with reports that MMR factors are upstream of IgH DSB formation (Schrader et al., 2007; Péron et al., 2008). Our observations further suggest that at least some of the DSBs generated during CSR are orchestrated by MLH1 through its ATPase activity. One possibility is that the ATPase-dependent conformational

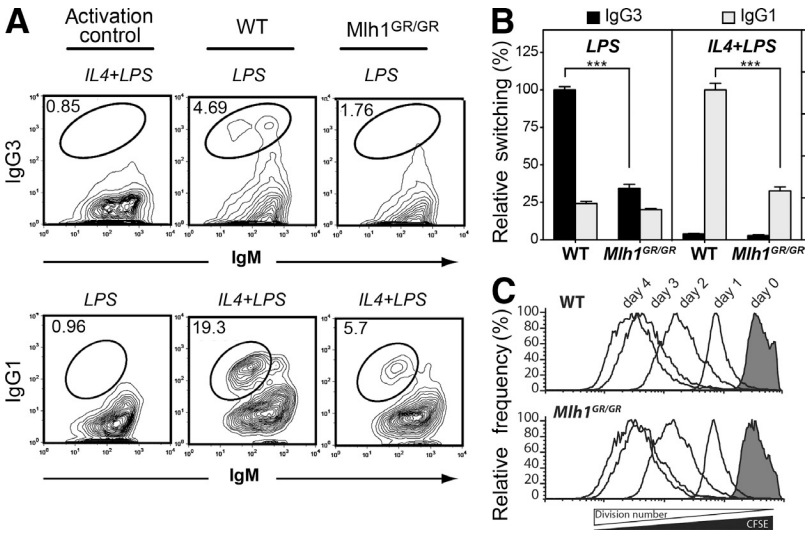

Figure 2. Splenic B cells from *Mlh1*$^{GR/GR}$ mice show decreased switching efficiencies in ex vivo cultures. (A) Representative FACS results from WT and *Mlh1*$^{GR/GR}$ cells stimulated with LPS or LPS + IL4 for 4 d. Percentages of switched cells are indicated within the gates. (B) The mean efficiency of switching in the WT group within each experiment was defined as 100%. Mean percentages of switching ± SEM are shown. Significance was determined using the two-tailed unpaired Student's *t* test (***, $P < 0.001$). Data correspond to six WT and seven *Mlh1*$^{GR/GR}$ mice assayed in two different experiments. (C) Overlay histograms of intracellular CFSE signal from splenic B cells stimulated with LPS + IL4 for different periods of time.

changes of MLH1 are important to activate PMS2 endonuclease (Pillon et al., 2010; Polosina and Cupples, 2010), allowing MutLα to introduce additional nicks into the SRs and thus facilitating the generation of DSBs in an attempt to repair the recurrent AID-induced mismatches. In fact, this is consistent with our recent report that the endonuclease activity of PMS2 is a major function of the MutLα complex during CSR (van Oers et al., 2010).

Microhomology-mediated end joining mechanisms are enhanced in *Mlh1*$^{GR/GR}$ switching B cells

The lack of MMR function and the reduction of DSBs have been attributed to delayed recombination efficiencies and differences in the length of microhomologies detected at the switch junctions (Lieber, 2010; Stavnezer et al., 2010). The use of long microhomologies during CSR has been interpreted to suggest that the alternate pathway of NHEJ (alt-NHEJ) is being used, and so the analysis of S-S junctions has been proven to be very informative of the role of end-joining factors (Yan et al., 2007; Kotnis et al., 2009). To determine the nature of the DSB repair pathway or pathways during CSR in activated *Mlh1*$^{GR/GR}$ B cells, we analyzed recombined switch junctions. We activated control and *Mlh1*$^{GR/GR}$ splenic B cells with LPS for 96 h and then amplified and sequenced Sμ-Sγ3 junctions. The distribution of breakpoints within the SRs was similar when distances up to 1 kb from the edges of the Sμ-Sγ3 amplicon were explored (Fig. 4 A). In contrast, comparison of the actual recombination sites between the Sμ and Sγ3 regions from mutant B cells to those of controls revealed profound differences. WT sequences contained ∼20% direct (blunt) junctions and only a few insertions, with most of the remainder being short microhomology junctions (1.64 bp mean; Fig. 4, B and C). In contrast, only 5% of direct junctions and also few insertions were found in *Mlh1*$^{GR/GR}$ B cells, which showed more junctions with longer microhomologies (5.45 bp mean) than the WT cells ($P < 0.0001$; Fig. 4, B and C).

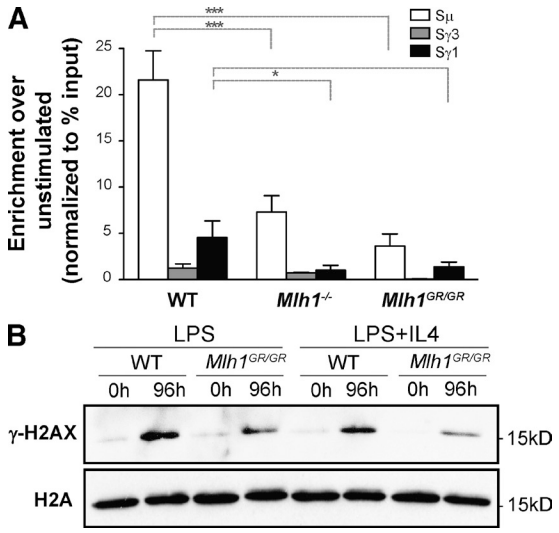

Figure 3. Impaired generation of DSBs in switching *Mlh1*$^{GR/GR}$ B cells. (A) ChIP experiments using anti-53BP1 antibodies were conducted on WT, *Mlh1*$^{-/-}$, and *Mlh1*$^{GR/GR}$ splenic B cells activated with LPS + IL4 for 50 h. Specific DNA fragments corresponding to the Sμ, Sγ3, and Sγ1 regions of the IgH locus were quantitated in the immunoprecipitates by real-time PCR relative to input DNA. The bars denote the enrichment of specific DNA fragments present in the corresponding immunoprecipitates in stimulated (t = 50 h) over unstimulated (t = 0 h) cells. Error bars indicate the SD of triple PCRs (*, $P < 0.05$; ***, $P < 0.001$). (B) Western blotting analysis was performed on WT and *Mlh1*$^{GR/GR}$ splenic B cells activated with either LPS (left) or with LPS + IL4 (right) for 96 h. Levels of γ-H2AX and anti-H2A were compared between the unstimulated (t = 0 h) and stimulated (t = 96 h) cells in the respective genotypes. A representative of three separate experiments is shown.

Our finding that sequence microhomology at Sμ-Sγ3 junctions is greater in *Mlh1*$^{GR/GR}$ switching B cells than in WT suggests a deficiency in canonical NHEJ in MLH1 mutant B cells and provides additional information regarding the role of MLH1 during the DNA end processing of SRs. The use of long microhomologies is unusual in canonical NHEJ at CSR junctions and suggests the participation of alt-NHEJ (Yan et al., 2007; Kotnis et al., 2009). This has been suggested to be the result of additional end processing of DSBs or the impaired recruitment of NHEJ proteins in the absence of MLH1–PMS2 proteins (Stavnezer et al., 2010). In fact, DNA helicases and other DNA repair factors have been shown to be part of the MutLα interactome (Cannavo et al., 2007) and may require the ATPase activity of MutLα for recruitment to the complex. More specifically, these interactome studies have identified EXO1 and DNA-PKcs as partners of MLH1, both of which have been shown to function during CSR in B cells (Stavnezer et al., 2010). EXO1 is not only an exonuclease member of the MMR complex but has also been shown to be involved in DNA end resection downstream of a DSB, whereas DNA-PKcs is a kinase protein integral for the mediation of DSB repair using the canonical NHEJ pathway (Kotnis et al., 2009; Lieber, 2010; Chahwan et al., 2011). During MMR, MutLα plays a role in the termination of EXO1-mediated strand excision by RPA (Genschel and Modrich, 2009). It is possible that the defect in the ATPase activity of MutLα interferes with this activity also during DNA end processing of SRs, which might lead to longer excision tracts and increased use of microhomologies during NHEJ.

Increased mutation frequencies at Sμ-Sγ3 junctions in *Mlh1*$^{GR/GR}$ switching B cells

Recombinant junctions usually accumulate mutations at the donor Sμ and acceptor Sγ regions (Stavnezer et al., 2010). To test whether the switching deficiencies observed in *Mlh1*$^{GR/GR}$ mice were accompanied by any alteration in SR mutations, we sequenced Sμ-Sγ3 junctions from LPS-activated mutant B cells. The comparison with WT sequences showed a significant increase in the overall frequency of mutations accumulated at the Sμ-Sγ3 junctions of *Mlh1*$^{GR/GR}$ B cells ($P < 0.01$; Fig. 4 D). This approximately twofold increase affected all types of mutations and hotspots in *Mlh1*$^{GR/GR}$ B cells

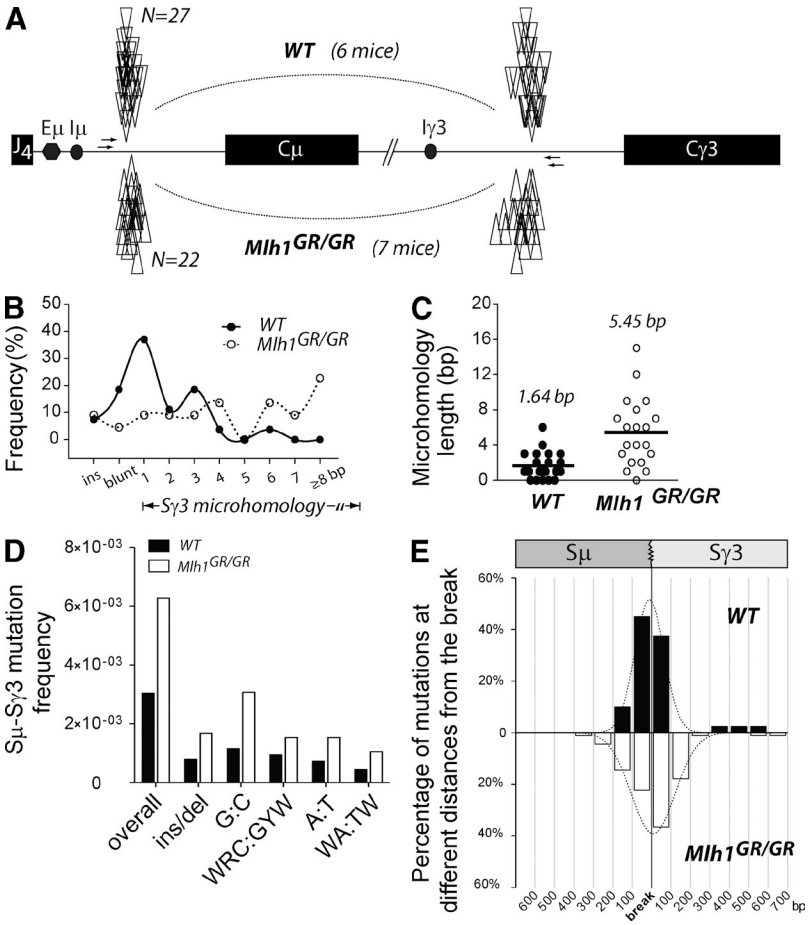

Figure 4. Increased microhomologies and mutation frequencies at Sμ–Sγ3 junctions in *Mlh1*$^{GR/GR}$ switching B cells. (A) Distribution of breakpoints (open triangles) within Sμ and Sγ3 SRs from 27 and 22 successful recombination events in six WT and seven *Mlh1*$^{GR/GR}$ mice, respectively. Arrows indicate the position of the nested primers used to detect Sμ-Sγ3 junctions. (B) Percentage of junctions exhibiting insertions (ins), blunt joins, or microhomologies. (C) Scatter plot representing the length in base pairs of each detected microhomology. Horizontal bars indicate the mean length of microhomology. (D) Frequency and type of mutations accumulated at the Sμ-Sγ3 junctions of WT and *Mlh1*$^{GR/GR}$ B cells. Insertions and deletions (ins/del) were computed together. WRC:GYW and WA:TW motifs (W = A or T; R = purine; Y = pyrimidine) correspond to preferred AID and error-prone polymerase Polη hotspots, respectively. (E) Distribution of mutations around the recombination breakpoints. Mutations occurring within the same bin window of 100 bp were counted together and represented in histograms.

(Fig. 4 D), but it did not affect the distribution of mutations around the recombination breaks, which was comparable in both mutant and WT sequences (Fig. 4 E).

The fact that *Mlh1*$^{GR/GR}$ B cells accumulate higher frequencies of mutations at the SRs seems consistent with the notion that deficiencies in MLH1 compromise the genome integrity of the cell and the efficiency of MMR mechanisms (Kunkel and Erie, 2005; Iyer et al., 2006; Jiricny, 2006). Because the frequency of switching was reduced to ∼30% that of WT cells (Fig. 2), it is possible that the defect in MLH1 slowed the recombination processes in most SRs and led to futile cycles of repair, which would allow the accumulation of additional AID hits and error-prone repair in a continuous attempt to progress through CSR.

Supported by all of these arguments, we therefore propose that the ATPase domain of MLH1 appears to be functional both upstream by promoting the generation of DSBs and downstream of the AID-generated mismatches by recruiting NHEJ factors and/or limiting EXO1-mediated resection. Our results cannot distinguish between these two latter alternatives but strongly suggest that the orchestration of the end-repair mechanisms downstream of the DSB require not only the scaffolding functions of MLH1 and PMS2 but also the ATPase activity of MLH1. It should be noted that the loss of the endonuclease activity of PMS2 did not affect the preferential use of canonical NHEJ (van Oers et al., 2010), whereas alt-NHEJ with its longer microhomologies appears to be favored in the *Mlh1*$^{GR/GR}$ B cells studied here. Therefore, the MLH1GR mutation does not only result in the loss of activation of the latent endonuclease of PMS2 but also must result in the loss of additional functions of MLH1.

It is becoming clearer that MMR factors can have separate scaffolding and catalytic functions, which could explain the distinct roles of these proteins during MMR processes. In this sense, mouse models representing separation of function mutations have proven to be useful in exploring the multiple roles of MMR protein complexes during error-free DNA repair, error-prone SHM, or DSB-mediated CSR (Chahwan et al., 2011). The role of the endonuclease activity of PMS2 during CSR was separated from the scaffolding functions of MutLα in the *Pms2*$^{EK/EK}$ mice (van Oers et al., 2010). Here, we suggest that MLH1 has ATPase-dependent functions that influence both the generation and the NHEJ repair of DSBs at the SRs. In contrast, other ATPase-independent functions of MLH1, such as those involved in the apoptotic response to DNA damage, are retained in the mutant *MLH1*$^{GR/GR}$ but not in the null mice (Avdievich et al., 2008). Therefore, some MLH1 functions are independent of its ATPase activity and seem to be irrelevant to CSR because they are not sufficient to enable moderate or normal efficiencies of switching in *Mlh1*$^{GR/GR}$ mice.

MATERIALS AND METHODS

Mice. The *Mlh1*$^{-/-}$ mice were generated previously by deleting exon 2 of the *Mlh1* gene (Edelmann et al., 1996). The *Mlh1*$^{G67R/G67R}$ mice were generated more recently and carry a missense mutation within exon 2 of the *Mlh1* gene (Avdievich et al., 2008). The G67R mutation slightly reduced

the levels of the mutant MLH1 protein, but this effect was very modest and did not affect the interaction of MLH1 with its MutLα partner PMS2 (Avdievich et al., 2008). All mouse experiments were approved by the Albert Einstein College of Medicine Animal Use Committee.

Immunizations and SHM assay. To analyze the V_H186.2 region, three 8-wk-old *Mlh1*$^{G67R/G67R}$ mice along with three WT littermates were immunized intraperitoneally with 200 μg NP_{36}-CGG (Biosearch Technologies) in alum (Thermo Fisher Scientific). To analyze the Jh2-Jh4 region, two aged mice (>8 mo) per genotype were used. In both cases, splenic B cells were purified to analyze SHM as previously described (Roa et al., 2010). Alignment and analysis of unique mutations were performed using SeqMan (DNASTAR) and SHMTool (MacCarthy et al., 2009). As consensus sequences, GenBank/EMBL/DDBJ no. J00530.1 (nucleotides 224–496) for V_H186.2, GenBank no. NT_039551.8 (nucleotides 25620771–25619943) for Jh2-Jh4, and GenBank no. NT_039551.8 (nucleotides 25521839–25521801) for the rearranged IgG1 constant region were used. The presence of significant A>>T and W<u>A</u>>><u>T</u>W bias in the WT sequences was used as a quality assessment of mutation datasets (Steele, 2009).

Ex vivo CSR assay. After depletion of T cells by complement-mediated lysis, splenic B cells were obtained from six WT and seven *Mlh1*$^{G67R/G67R}$ 8-wk-old mice. Purified B cells were plated at a concentration of 0.5×10^6 cells/ml and stimulated with either 50 μg/ml LPS (Sigma-Aldrich) or 50 μg/ml LPS and 50 ng/ml rIL-4 (R&D Systems) for 4 d. Simultaneously, purified splenic B cells were stained with 10 μM CFSE (Invitrogen) in PBS/0.1% BSA at a final concentration of 10^7 cells/ml. At various time points after stimulation, cells were harvested and fixed with 1% paraformaldehyde in PBS to evaluate cellular proliferation. Surface IgM, IgG1, and IgG3 and intracellular CFSE were analyzed with a FACSCalibur (BD) and FlowJo software (Tree Star).

Analysis of Sμ-Sγ3 switch junctions. Genomic DNA was prepared from splenic B cells cultured for 4 d with 50 μg/ml LPS to induce specific switching from IgM to IgG3. Junctional Sμ-Sγ3 DNA was amplified using high-fidelity *PfuTurbo* DNA polymerase (Agilent Technologies) as previously described (van Oers et al., 2010). Alignment and analysis of sequenced switch junctions were performed using BLAST2seq (NCBI) with the low-complexity filter disabled. Sequences from GenBank accession no. NC_000078.6 were used as SR consensus sequences. Microhomology was defined as matched successive nucleotides that cannot be uniquely assigned to either germline Sμ or Sγ3 consensus sequences.

Western blotting and quantitative ChIP. For Western blot analysis, 1.0×10^6 cells were lysed in Laemmli sample buffer followed by DNA shearing using a syringe. After boiling for 5 min, samples were loaded on 4–20% polyacrylamide gels followed by immunoblotting according to the manufacturer's specification as described previously (Ramachandran et al., 2010). ChIP was performed according to published protocols (Kuang et al., 2009). In brief, sonicated chromatin from 2.0×10^6 purified splenic B cells was preincubated for 2 h at 4°C with Protein A–agarose beads (Roche) to avoid nonspecific binding. After centrifugation at maximum speed at 4°C for 5 min, the supernatant was incubated overnight at 4°C with 2 μg 53BP1 antisera (Novus Biologicals). The mixture was then centrifuged as in the preceding step, and chromatin–antibody complexes were collected by incubation with Protein A–agarose beads for 90 min at 4°C. Washes and isolation of DNA, as well as quantitative PCR conditions and primers are described previously (Kuang et al., 2009).

This work was supported by Postdoctoral Fellowship EX-2006-0732 from the Spanish Ministry of Education and Science (to S. Roa) and National Institutes of Health grants R01CA72649 and R01CA102705 (to M.D. Scharff) and R01CA76329 and R01CA93484 (to W. Edelmann). M.D. Scharff is supported by the Harry Eagle Chair provided by the National Women's Division of the Albert Einstein College of Medicine.

The authors have no conflicting financial interests.

Submitted: 25 July 2011
Accepted: 2 March 2012

REFERENCES

Avdievich, E., C. Reiss, S.J. Scherer, Y. Zhang, S.M. Maier, B. Jin, H. Hou Jr., A. Rosenwald, H. Riedmiller, R. Kucherlapati, et al. 2008. Distinct effects of the recurrent Mlh1G67R mutation on MMR functions, cancer, and meiosis. *Proc. Natl. Acad. Sci. USA*. 105:4247–4252. http://dx.doi.org/10.1073/pnas.0800276105

Ban, C., M. Junop, and W. Yang. 1999. Transformation of MutL by ATP binding and hydrolysis: a switch in DNA mismatch repair. *Cell*. 97:85–97. http://dx.doi.org/10.1016/S0092-8674(00)80717-5

Bergerat, A., B. de Massy, D. Gadelle, P.C. Varoutas, A. Nicolas, and P. Forterre. 1997. An atypical topoisomerase II from Archaea with implications for meiotic recombination. *Nature*. 386:414–417. http://dx.doi.org/10.1038/386414a0

Bothmer, A., D.F. Robbiani, M. Di Virgilio, S.F. Bunting, I.A. Klein, N. Feldhahn, J. Barlow, H.T. Chen, D. Bosque, E. Callen, et al. 2011. Regulation of DNA end joining, resection, and immunoglobulin class switch recombination by 53BP1. *Mol. Cell*. 42:319–329. http://dx.doi.org/10.1016/j.molcel.2011.03.019

Cannavo, E., B. Gerrits, G. Marra, R. Schlapbach, and J. Jiricny. 2007. Characterization of the interactome of the human MutL homologues MLH1, PMS1, and PMS2. *J. Biol. Chem*. 282:2976–2986. http://dx.doi.org/10.1074/jbc.M609989200

Chahwan, R., W. Edelmann, M.D. Scharff, and S. Roa. 2011. Mismatch-mediated error prone repair at the immunoglobulin genes. *Biomed. Pharmacother.* 65:529–536. http://dx.doi.org/10.1016/j.biopha.2011.09.001

Dutta, R., and M. Inouye. 2000. GHKL, an emergent ATPase/kinase superfamily. *Trends Biochem. Sci*. 25:24–28. http://dx.doi.org/10.1016/S0968-0004(99)01503-0

Eccleston, J., C. Yan, K. Yuan, F.W. Alt, and E. Selsing. 2011. Mismatch repair proteins MSH2, MLH1, and EXO1 are important for class-switch recombination events occurring in B cells that lack nonhomologous end joining. *J. Immunol*. 186:2336–2343. http://dx.doi.org/10.4049/jimmunol.1003104

Edelmann, W., P.E. Cohen, M. Kane, K. Lau, B. Morrow, S. Bennett, A. Umar, T. Kunkel, G. Cattoretti, R. Chaganti, et al. 1996. Meiotic pachytene arrest in MLH1-deficient mice. *Cell*. 85:1125–1134. http://dx.doi.org/10.1016/S0092-8674(00)81312-4

Ehrenstein, M.R., C. Rada, A.M. Jones, C. Milstein, and M.S. Neuberger. 2001. Switch junction sequences in PMS2-deficient mice reveal a microhomology-mediated mechanism of Ig class switch recombination. *Proc. Natl. Acad. Sci. USA*. 98:14553–14558. http://dx.doi.org/10.1073/pnas.241525998

Genschel, J., and P. Modrich. 2009. Functions of MutLalpha, replication protein A (RPA), and HMGB1 in 5′-directed mismatch repair. *J. Biol. Chem*. 284:21536–21544. http://dx.doi.org/10.1074/jbc.M109.021287

Hu, X., M. Machius, and W. Yang. 2003. Monovalent cation dependence and preference of GHKL ATPases and kinases. *FEBS Lett*. 544:268–273. http://dx.doi.org/10.1016/S0014-5793(03)00519-2

Iyer, R.R., A. Pluciennik, V. Burdett, and P.L. Modrich. 2006. DNA mismatch repair: functions and mechanisms. *Chem. Rev*. 106:302–323. http://dx.doi.org/10.1021/cr0404794

Jiricny, J. 2006. The multifaceted mismatch-repair system. *Nat. Rev. Mol. Cell Biol*. 7:335–346. http://dx.doi.org/10.1038/nrm1907

Johnson, J.R., N. Erdeniz, M. Nguyen, S. Dudley, and R.M. Liskay. 2010. Conservation of functional asymmetry in the mammalian MutLα ATPase. *DNA Repair (Amst.)*.9:1209–1213.http://dx.doi.org/10.1016/j.dnarep.2010.08.006

Kim, N., G. Bozek, J.C. Lo, and U. Storb. 1999. Different mismatch repair deficiencies all have the same effects on somatic hypermutation: Intact primary mechanism accompanied by secondary modifications. *J. Exp. Med*. 190:21–30. http://dx.doi.org/10.1084/jem.190.1.21

Kotnis, A., L. Du, C. Liu, S.W. Popov, and Q. Pan-Hammarström. 2009. Non-homologous end joining in class switch recombination: the beginning of the end. *Philos. Trans. R. Soc. Lond. B Biol. Sci*. 364:653–665. http://dx.doi.org/10.1098/rstb.2008.0196

Kuang, F.L., Z. Luo, and M.D. Scharff. 2009. H3 trimethyl K9 and H3 acetyl K9 chromatin modifications are associated with class switch recombination. *Proc. Natl. Acad. Sci. USA*. 106:5288–5293. http://dx.doi.org/10.1073/pnas.0901368106

Kunkel, T.A., and D.A. Erie. 2005. DNA mismatch repair. *Annu. Rev. Biochem*. 74:681–710. http://dx.doi.org/10.1146/annurev.biochem.74.082803.133243

Lieber, M.R. 2010. The mechanism of double-strand DNA break repair by the nonhomologous DNA end-joining pathway. *Annu. Rev. Biochem*. 79:181–211. http://dx.doi.org/10.1146/annurev.biochem.052308.093131

MacCarthy, T., S. Roa, M.D. Scharff, and A. Bergman. 2009. SHMTool: a webserver for comparative analysis of somatic hypermutation datasets. *DNA Repair (Amst.)*. 8:137–141. http://dx.doi.org/10.1016/j.dnarep.2008.09.006

Maul, R.W., H. Saribasak, S.A. Martomo, R.L. McClure, W. Yang, A. Vaisman, H.S. Gramlich, D.G. Schatz, R. Woodgate, D.M. Wilson III, and P.J. Gearhart. 2011. Uracil residues dependent on the deaminase AID in immunoglobulin gene variable and switch regions. *Nat. Immunol*. 12:70–76. http://dx.doi.org/10.1038/ni.1970

Péron, S., A. Metin, P. Gardès, M.A. Alyanakian, E. Sheridan, C.P. Kratz, A. Fischer, and A. Durandy. 2008. Human PMS2 deficiency is associated with impaired immunoglobulin class switch recombination. *J. Exp. Med*. 205:2465–2472. http://dx.doi.org/10.1084/jem.20080789

Phung, Q.H., D.B. Winter, R. Alrefai, and P.J. Gearhart. 1999. Hypermutation in Ig V genes from mice deficient in the MLH1 mismatch repair protein. *J. Immunol*. 162:3121–3124.

Pillon, M.C., J.J. Lorenowicz, M. Uckelmann, A.D. Klocko, R.R. Mitchell, Y.S. Chung, P. Modrich, G.C. Walker, L.A. Simmons, P. Friedhoff, and A. Guarné. 2010. Structure of the endonuclease domain of MutL: unlicensed to cut. *Mol. Cell*. 39:145–151. http://dx.doi.org/10.1016/j.molcel.2010.06.027

Polosina, Y.Y., and C.G. Cupples. 2010. MutL: conducting the cell's response to mismatched and misaligned DNA. *Bioessays*. 32:51–59. http://dx.doi.org/10.1002/bies.200900089

Raevaara, T.E., M.K. Korhonen, H. Lohi, H. Hampel, E. Lynch, K.E. Lönnqvist, E. Holinski-Feder, C. Sutter, W. McKinnon, S. Duraisamy, et al. 2005. Functional significance and clinical phenotype of nontruncating mismatch repair variants of MLH1. *Gastroenterology*. 129:537–549.

Ramachandran, S., R. Chahwan, R.M. Nepal, D. Frieder, S. Panier, S. Roa, A. Zaheen, D. Durocher, M.D. Scharff, and A. Martin. 2010. The RNF8/RNF168 ubiquitin ligase cascade facilitates class switch recombination. *Proc. Natl. Acad. Sci. USA*. 107:809–814. http://dx.doi.org/10.1073/pnas.0913790107

Räschle, M., P. Dufner, G. Marra, and J. Jiricny. 2002. Mutations within the hMLH1 and hPMS2 subunits of the human MutLalpha mismatch repair factor affect its ATPase activity, but not its ability to interact with hMutSalpha. *J. Biol. Chem*. 277:21810–21820. http://dx.doi.org/10.1074/jbc.M108787200

Roa, S., Z. Li, J.U. Peled, C. Zhao, W. Edelmann, and M.D. Scharff. 2010. MSH2/MSH6 complex promotes error-free repair of AID-induced dU:G mispairs as well as error-prone hypermutation of A:T sites. *PLoS ONE*. 5:e11182. http://dx.doi.org/10.1371/journal.pone.0011182

Rogakou, E.P., C. Boon, C. Redon, and W.M. Bonner. 1999. Megabase chromatin domains involved in DNA double-strand breaks in vivo. *J. Cell Biol*. 146:905–916. http://dx.doi.org/10.1083/jcb.146.5.905

Sacho, E.J., F.A. Kadyrov, P. Modrich, T.A. Kunkel, and D.A. Erie. 2008. Direct visualization of asymmetric adenine-nucleotide-induced conformational changes in MutL alpha. *Mol. Cell*. 29:112–121. http://dx.doi.org/10.1016/j.molcel.2007.10.030

Schrader, C.E., W. Edelmann, R. Kucherlapati, and J. Stavnezer. 1999. Reduced isotype switching in splenic B cells from mice deficient in mismatch repair enzymes. *J. Exp. Med*. 190:323–330. http://dx.doi.org/10.1084/jem.190.3.323

Schrader, C.E., J.E. Guikema, E.K. Linehan, E. Selsing, and J. Stavnezer. 2007. Activation-induced cytidine deaminase-dependent DNA breaks in class switch recombination occur during G1 phase of the cell cycle and depend upon mismatch repair. *J. Immunol*. 179:6064–6071.

Shah, S.N., S.E. Hile, and K.A. Eckert. 2010. Defective mismatch repair, microsatellite mutation bias, and variability in clinical cancer phenotypes. *Cancer Res*. 70:431–435. http://dx.doi.org/10.1158/0008-5472.CAN-09-3049

Spampinato, C., and P. Modrich. 2000. The MutL ATPase is required for mismatch repair. *J. Biol. Chem*. 275:9863–9869. http://dx.doi.org/10.1074/jbc.275.13.9863

Stavnezer, J. 2011. Complex regulation and function of activation-induced cytidine deaminase. *Trends Immunol*. 32:194–201. http://dx.doi.org/10.1016/j.it.2011.03.003

Stavnezer, J., A. Björkman, L. Du, A. Cagigi, and Q. Pan-Hammarström. 2010. Mapping of switch recombination junctions, a tool for studying DNA repair pathways during immunoglobulin class switching. *Adv. Immunol*. 108:45–109. http://dx.doi.org/10.1016/B978-0-12-380995-7.00003-3

Steele, E.J. 2009. Mechanism of somatic hypermutation: critical analysis of strand biased mutation signatures at A:T and G:C base pairs. *Mol. Immunol*. 46:305–320. http://dx.doi.org/10.1016/j.molimm.2008.10.021

Tomer, G., A.B. Buermeyer, M.M. Nguyen, and R.M. Liskay. 2002. Contribution of human mlh1 and pms2 ATPase activities to DNA mismatch repair. *J. Biol. Chem*. 277:21801–21809. http://dx.doi.org/10.1074/jbc.M111342200

van Oers, J.M., S. Roa, U. Werling, Y. Liu, J. Genschel, H. Hou Jr., R.S. Sellers, P. Modrich, M.D. Scharff, and W. Edelmann. 2010. PMS2 endonuclease activity has distinct biological functions and is essential for genome maintenance. *Proc. Natl. Acad. Sci. USA*. 107:13384–13389. http://dx.doi.org/10.1073/pnas.1008589107

Yan, C.T., C. Boboila, E.K. Souza, S. Franco, T.R. Hickernell, M. Murphy, S. Gumaste, M. Geyer, A.A. Zarrin, J.P. Manis, et al. 2007. IgH class switching and translocations use a robust non-classical end-joining pathway. *Nature*. 449:478–482. http://dx.doi.org/10.1038/nature06020